

NASA TECHNICAL NOTE



NASA TN D-2206

6.1

LOAN COPY
JUL 1967
KIRTLAND AFB, N.M.



NASA TN D-2206

**ANALYSIS OF PLASTIC THERMAL STRESSES
AND STRAINS IN FINITE THIN PLATE
OF STRAIN-HARDENING MATERIAL**

by Ernest Roberts, Jr., and Alexander Mendelson

*Lewis Research Center
Cleveland, Ohio*

ANALYSIS OF PLASTIC THERMAL STRESSES AND STRAINS IN
FINITE THIN PLATE OF STRAIN-HARDENING MATERIAL

By Ernest Roberts, Jr., and Alexander Mendelson

Lewis Research Center
Cleveland, Ohio

NATIONAL AERONAUTICS AND SPACE ADMINISTRATION

For sale by the Office of Technical Services, Department of Commerce,
Washington, D.C. 20230 -- Price \$0.75



ANALYSIS OF PLASTIC THERMAL STRESSES AND STRAINS IN
FINITE THIN PLATE OF STRAIN-HARDENING MATERIAL

by Ernest Roberts, Jr., and Alexander Mendelson

Lewis Research Center

SUMMARY

A practical method for obtaining the plastic deformations in a biaxial stress field is presented. The method is numerical, utilizing a system of successive approximations. There are no limitations regarding boundaries, loading history, stress-strain curves, or temperature dependence of material properties. The incremental theory of plasticity is used. Two examples are presented for strain-hardening materials: a thermally loaded long rectangular plate, and a thermally loaded square plate. Where possible, comparisons are made with existing solutions. The validity of certain approximations to the solution is also investigated.

INTRODUCTION

There is currently considerable interest in stress analysis of structures that have been permitted to deform plastically. Certain statically loaded structures, some pressure vessels, for example, can be permitted to deform to beyond the elastic limit without limiting their usefulness. Furthermore, the life of cyclically loaded structures has been shown to depend on the amount of plastic flow per cycle (ref. 1). Available solutions, however, are limited to one-dimensional stress fields or neglect strain-hardening or both.

There are several closed-form solutions to elementary problems using ideally plastic materials (ref. 2) and a few for strain-hardening materials (ref. 3), but they are confined to one-dimensional stress fields. The numerical procedure developed in reference 4 permits solutions to a much wider variety of one-dimensional problems with strain-hardening by using successive approximations. Some two-dimensional problems have been solved in reference 5 by using finite-difference techniques, but these neglect strain-hardening.

A method is described that combines the established numerical techniques of finite differences with the successive approximation technique of reference 4 to obtain an accurate solution to two-dimensional plane-stress or plane-strain problems for a plastically deforming work-hardening material. The only assumptions necessary are the usual ones for plane-elastostatic problem, the classical conditions of continuity, homogeneity, isotropy, and those assumptions

associated with numerical differentiation. In the illustrative examples rectangular boundaries are assumed together with linear strain hardening and material properties independent of temperature. These restrictions, however, are not intrinsic to the present method. The method may easily be extended to more complicated boundaries, stress-strain curves, and material properties.

The report presents the solution to two problems: a thermally loaded long rectangular plate, which is essentially a one-dimensional problem, and a thermally loaded square plate, which is a two-dimensional problem. The treatment of this report uses a stress-strain curve representative of strain-hardening materials, the von Mises yield criterion, and its associated flow rule, which results in the Prandtl-Reuss stress-strain relations; that is, the so called incremental theory of plasticity is used. Comparisons were made with other solutions, where they exist, and were found to be in good agreement. The problems were chosen to illustrate the use of the method and are not indicative of any limitations regarding boundaries, loading, stress-strain curves, or material properties.

SYMBOLS

E	Young's modulus
g	function of plastic-strain increments
k_1	constant of proportionality defining temperature function
m	dimensionless tangent modulus
n	integer
T	temperature function
x	spanwise coordinate
y	chordwise coordinate
z	thickness coordinate
α	linear coefficient of thermal expansion
β	span-to-chord ratio
γ	shear strain
ϵ	normal strain
λ	constant
ν	Poisson's ratio
σ	normal stress

τ shear stress

ϕ Airy's stress function

∇^2 harmonic operator, $\frac{\partial^2}{\partial x^2} + \frac{\partial^2}{\partial y^2}$

∇^4 biharmonic operator, $\frac{\partial^4}{\partial x^4} + 2 \frac{\partial^4}{\partial x^2 \partial y^2} + \frac{\partial^4}{\partial y^4}$

Subscripts:

e equivalent or effective

i row index

j column index

p plastic component

t total

x spanwise coordinate

y chordwise coordinate

z thickness coordinate

Superscripts:

e elastic component

* dimensionless quantity

ANALYSIS

The problem of determining the elastic state of stress in a thin rectangular plate of uniform thickness is in the category of generalized plane-stress problems. Such problems are frequently stated in terms of Airy's stress function, whereby the problem is reduced to solving a single fourth-order partial differential equation (ref. 6). The method has been applied successfully to thermally loaded rectangular plates with numerical procedures being used to solve this partial differential equation with its associated boundary conditions (ref. 7). A similar differential equation can be derived for defining the plastic state of stress in such a plate from the conditions of equilibrium and compatibility and a set of stress-strain relations including plastic terms. The stress-strain relations with temperature terms and plastic-strain terms added are (in the coordinate system defined in fig. 1) as follows:

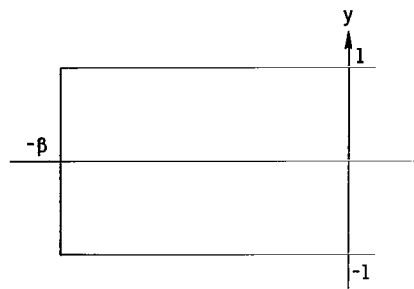


Figure 1. - Unnormalized coordinate system used to determine state of stress in thermally loaded thin flat plate.

$$\epsilon_x = \frac{1}{E} (\sigma_x - \nu \sigma_y) + \sum \Delta \epsilon_{x,p} + \Delta \epsilon_{x,p} + \alpha T \quad (1a)$$

$$\epsilon_y = \frac{1}{E} (\sigma_y - \nu \sigma_x) + \sum \Delta \epsilon_{y,p} + \Delta \epsilon_{y,p} + \alpha T \quad (1b)$$

$$\gamma = \frac{1 + \nu}{E} \tau + \sum \Delta \gamma_p + \Delta \gamma_p \quad (1c)$$

where the \sum 's represent the accumulation of plastic strain increments from the beginning of the loading history up to but not including the present increment.

The equilibrium and compatibility relations are

$$\frac{\partial}{\partial x} \sigma_x + \frac{\partial}{\partial y} \tau = 0 \quad (2a)$$

$$\frac{\partial}{\partial y} \sigma_y + \frac{\partial}{\partial x} \tau = 0 \quad (2b)$$

$$\frac{\partial^2}{\partial y^2} \epsilon_x + \frac{\partial^2}{\partial x^2} \epsilon_y - 2 \frac{\partial^2}{\partial x \partial y} \gamma = 0 \quad (3)$$

The incremental plasticity relations derived from the von Mises yield criterion and its associated flow rule, as presented in reference 2, are

$$\Delta \epsilon_{x,p} = \frac{\Delta \epsilon_{e,p}}{2\sigma_e} [2\sigma_x - \sigma_y] \quad (4a)$$

$$\Delta \epsilon_{y,p} = \frac{\Delta \epsilon_{e,p}}{2\sigma_e} [2\sigma_y - \sigma_x] \quad (4b)$$

$$\Delta \gamma_p = \frac{3 \Delta \epsilon_{e,p}}{2\sigma_e} \tau \quad (4c)$$

where

$$\Delta \epsilon_{e,p} \equiv \frac{2}{\sqrt{3}} \sqrt{\Delta \epsilon_{x,p}^2 + \Delta \epsilon_{y,p}^2 + \Delta \epsilon_{x,p} \Delta \epsilon_{y,p} + \Delta \gamma_p^2} \quad (5)$$

and

$$\sigma_e \equiv \sqrt{\sigma_x^2 + \sigma_y^2 - \sigma_x \sigma_y + 3\tau^2} \quad (6)$$

Finally, a relation is needed defining the stress-strain curve above the yield point. This relation depends on the material and need not be an explicit function. If plastic flow occurs during the increment of loading under consideration, the function can be written as follows:

$$\sigma_e = \sigma_0 + f\left(\sum \Delta\epsilon_{e,p}\right) \quad (7a)$$

For example, as can be seen from figure 2, for linear strain-hardening

$$f = E \frac{m}{1-m} \sum \Delta\epsilon_{e,p} \quad (7b)$$

Equations (1) to (7), along with the condition that all normal and shear stresses vanish on the boundaries, completely define this problem. The problem will be solved by combining equations (1) to (3) and by introducing a stress function. First the compatibility relation is expressed in terms of the stresses by combining equations (1) and (3). This process yields

$$\left(\frac{\partial^2}{\partial x^2} + \frac{\partial^2}{\partial y^2}\right) E\alpha T - 2(1+\nu) \frac{\partial^2}{\partial x \partial y} \tau + \frac{\partial^2}{\partial y^2} \sigma_x$$

$$+ \frac{\partial^2}{\partial x^2} \sigma_y - \nu \frac{\partial^2}{\partial y^2} \sigma_y - \nu \frac{\partial^2}{\partial x^2} \sigma_x + g = 0$$

where

$$g = E \left[\frac{\partial^2}{\partial y^2} \left(\sum \Delta\epsilon_{x,p} + \Delta\epsilon_{x,p} \right) + \frac{\partial^2}{\partial x^2} \left(\sum \Delta\epsilon_{y,p} + \Delta\epsilon_{y,p} \right) - 2 \frac{\partial^2}{\partial x \partial y} \left(\sum \Delta\gamma_p + \Delta\gamma_p \right) \right] \quad (8)$$

Introducing the stress function $\varphi = \varphi(x,y)$ defined by

$$\frac{\partial^2}{\partial y^2} \varphi = \sigma_x, \quad \frac{\partial^2}{\partial x^2} \varphi = \sigma_y, \quad - \frac{\partial^2}{\partial x \partial y} \varphi = \tau \quad (9)$$

and substituting into equation (8) yield

$$\nabla^4 \varphi + \nabla^2 E\alpha T + g = \nu \left(2 \frac{\partial^2}{\partial x \partial y} \tau + \frac{\partial^2}{\partial y^2} \sigma_y + \frac{\partial^2}{\partial x^2} \sigma_x \right) \quad (10)$$

Differentiating equation (2a) with respect to x and equation (2b) with respect to y and adding yield

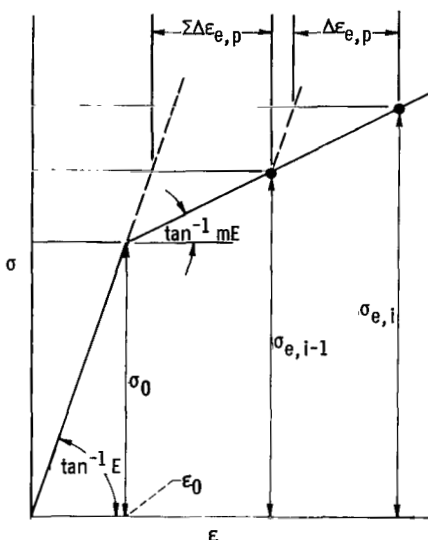


Figure 2. - Stress-strain curve for sample problem. Dimensionless tangent modulus, 0.1.

$$2 \frac{\partial^2}{\partial x \partial y} \tau + \frac{\partial^2}{\partial y^2} \alpha_y + \frac{\partial^2}{\partial x^2} \alpha_x = 0 \quad (11)$$

Substituting that expression into equation (10) produces the following partial differential equation that must be solved by using suitable boundary conditions:

$$\nabla^4 \phi + \nabla^2 E \alpha T + g = 0 \quad (12)$$

Boundary conditions for equation (12) derived from the vanishing of all normal and shear stresses on the boundaries are

$$\phi(x, 1) = 0 \quad (13a)$$

$$\frac{\partial}{\partial y} \phi(x, 1) = 0 \quad (13b)$$

$$\phi(\beta, y) = 0 \quad (13c)$$

$$\frac{\partial}{\partial x} \phi(\beta, y) = 0 \quad (13d)$$

Equation (12) is nonlinear, making a closed-form solution difficult to obtain; therefore, an iterative method is used in this paper. Iterative procedures have become commonplace in recent years with the increased use of high-speed electronic computing equipment. The differential equation is rewritten in difference-equation form at a large number of points in the rectangular region, and the resulting system of algebraic equations yields a value of ϕ at each point. The procedure used in so doing is described in appendix A.

Reference 4 utilizes a method of successive approximations, which is readily adapted to the present problem. It operates on the quantities equivalent plastic strain and equivalent stress, as defined in equations (5) and (6); these are the quantities in a uniaxially loaded system corresponding to the biaxial state of stress in a plane stress system. Briefly, the method is as follows:

- (1) Select a value of load.
- (2) Guess initial values of the plastic-strain increments.
- (3) Calculate the equivalent plastic-strain increment from equation (5).
- (4) Determine the value of σ_e from the stress-strain curve for the material.
- (5) Calculate g from equation (8) by using the current plastic-strain increments.
- (6) Solve equation (12) for the stress function.

(7) Calculate the stresses from equation (9).

(8) Calculate a new set of plastic-strain increments from equations (4).

(9) Repeat steps 3 to 8 until the newly calculated plastic-strain increments are sufficiently close to the previous ones. (Where there are no plastic strains, only one iteration is necessary.)

(10) Increment the load, sum the plastic-strain increments, and return to step 2.

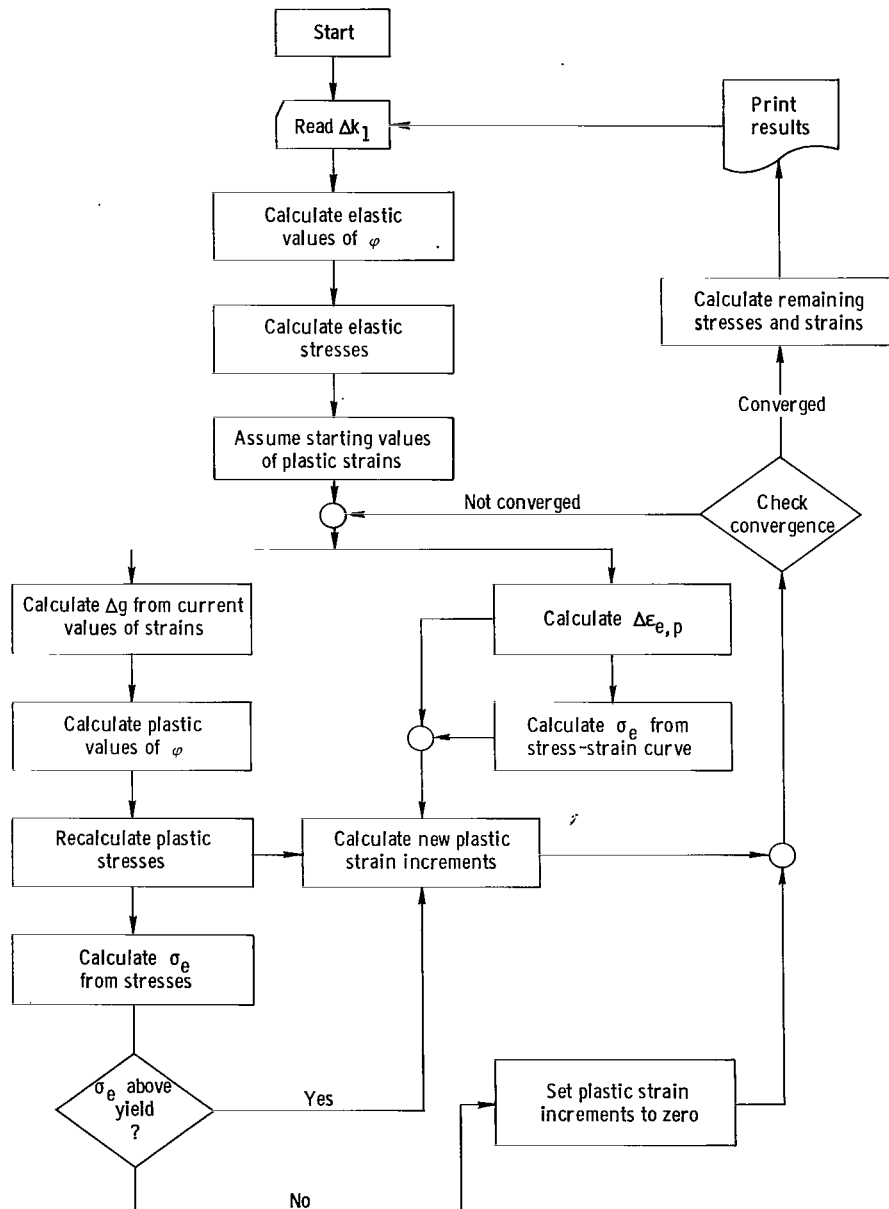


Figure 3. - Calculation procedure for iterative finite-difference method of solution.

This procedure may be applied only where there is no unloading. When unloading occurs, only the elastic component of the strain is recovered. Furthermore, on reloading, no additional plastic flow occurs until the stress at which unloading occurred is reached. The details of the computational procedure will not be discussed in this report.

It is to be noted that the values of stress produced by the above operations do not correspond to the value of equivalent stress determined from the stress-strain curve until convergence occurs. The procedure as described in the preceding paragraphs is outlined graphically in figure 3 (see p. 7).

DISCUSSION

The presentation of the solution to a problem, such as the one presented in this report, is of little value unless sufficient checks are available to instill a degree of confidence in its use. Fortunately, there are a few checks available for this problem. The solution for loads too small to produce plastic flow can be compared with the solutions presented in reference 8. That reference discusses the problem of an elastic flat plate of finite dimensions subjected to a chordwise thermal gradient. Reference 7 discusses a similarly loaded infinite strip. The solutions are identical along the central chord of long rectangular plates. For loads great enough to produce plastic flow, comparison can be made with the problem considered in reference 3. Reference 3 concerns itself with the semi-infinite plate, but by the principle of Saint-Venant that solution should be identical with the solution for a long rectangular plate far from its ends. Reference 8 verifies that statement in the elastic range for plates having span-to-chord ratios of 3 or greater. In summary, the following comparisons can be made for the two problems under consideration: for the rectangular plate the elastic solution everywhere and the plastic solution far from the ends can be checked against previous solutions; for the square plate the elastic solution everywhere can be compared with other solutions. All the comparisons will be made for the case of a parabolic chordwise temperature distribution $T^* = k_l y^2$, where T^* is a dimensionalized temperature function.

Figure 4 compares the elastic stress distribution in a 3 by 1 plate subjected to a chordwise parabolic temperature distribution with the solution presented in reference 8. The figures are presented in terms of a dimensionless stress, the ratio of the stress to the yield stress. Reference 8 uses the method of collocation to obtain the solution. It compares favorably with other solutions in the literature, and far from the ends agrees with the classical solution for an infinite strip. The figures show excellent agreement between the finite-difference solution and the collocation solution and give some confidence that a sufficiently small grid was chosen for the elastic finite-difference solution.

Figure 5 compares the plastic solution at midspan of the rectangular plate with the solution of reference 3. A strain-hardening material is assumed, with a dimensionless tangent modulus of 0.1, as shown in figure 2 (p. 5). Reference 3 gives the solution of the infinite strip. That solution also compares favorably with others in the literature. Unfortunately, the solution far from

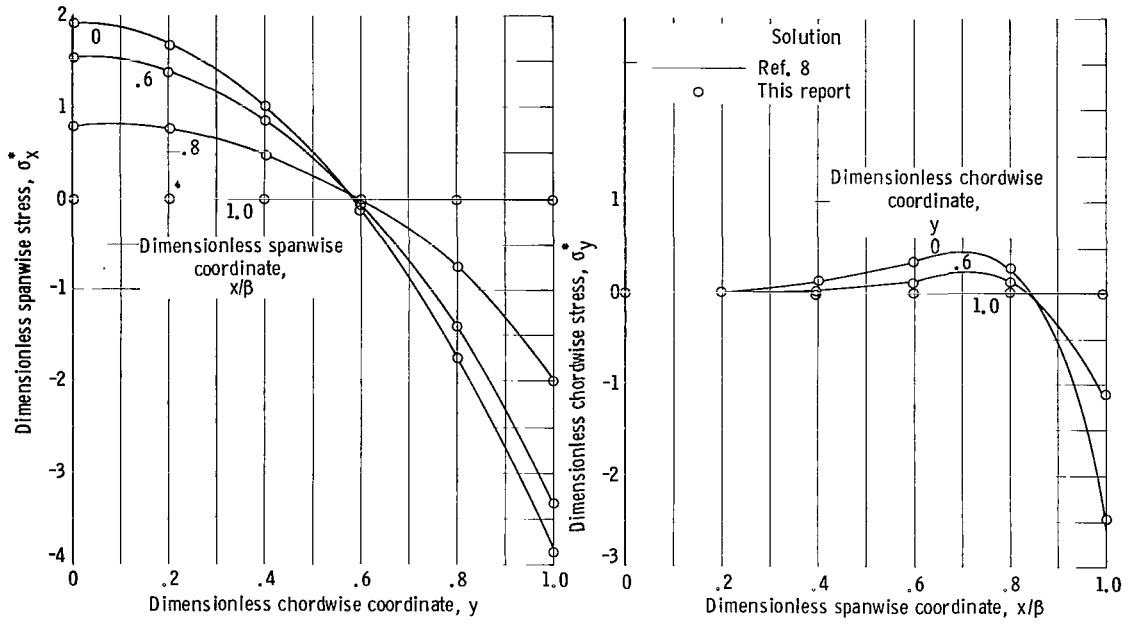


Figure 4. - Comparison of elastic stress solution in 3 by 1 plate with elastic solution of reference 8. Proportionality constant, 5.7; parabolic chordwise temperature distribution.

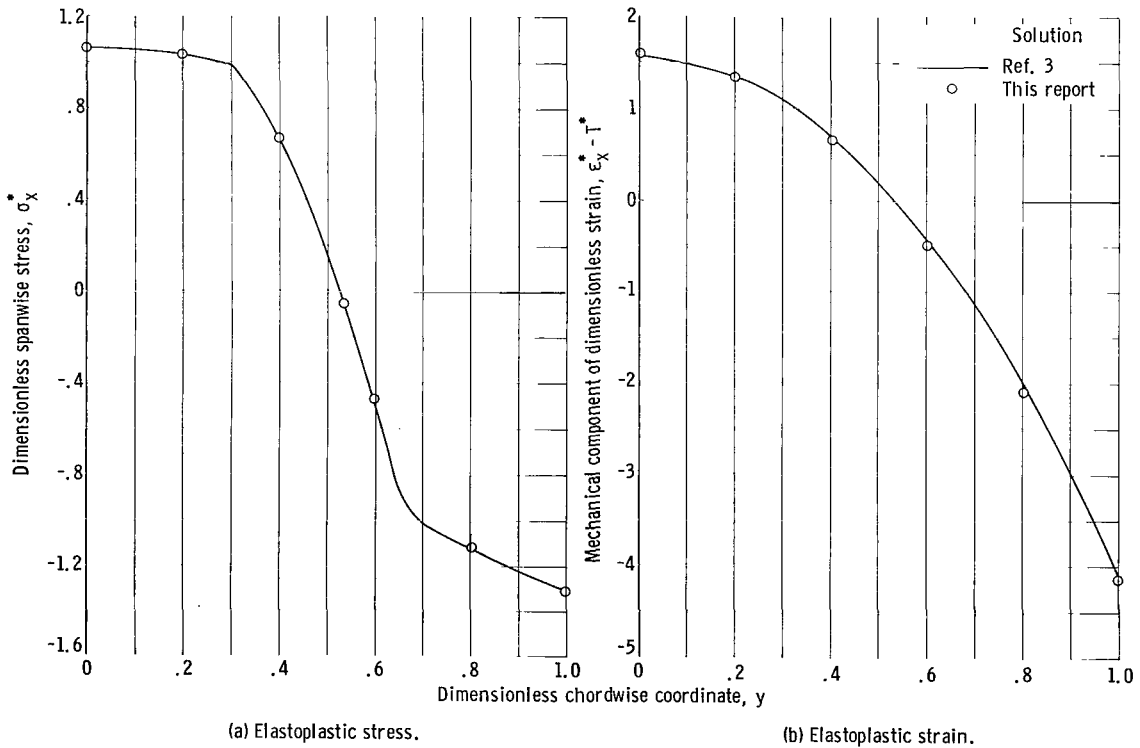


Figure 5. - Comparison of elastoplastic strain and stress solutions at midspan of 3 by 1 plate with solutions of infinite strip in reference 3; proportionality constant, 5.7; parabolic chordwise temperature distribution.

the ends is the only one available. But it can be seen that again the agreement between the two is excellent.

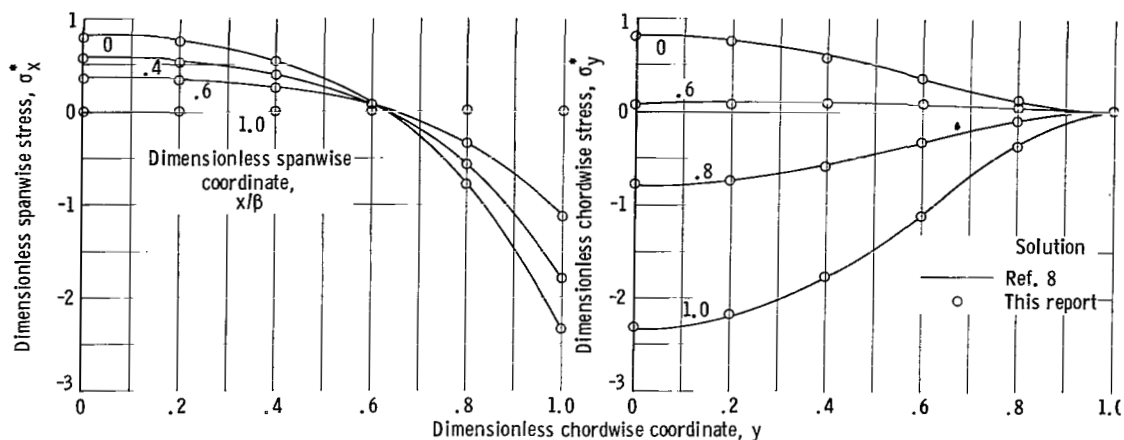


Figure 6. - Comparison of elastic-stress solution in square plate with elastic solution of reference 8. Proportionality constant, 5.7; parabolic chordwise temperature distribution.

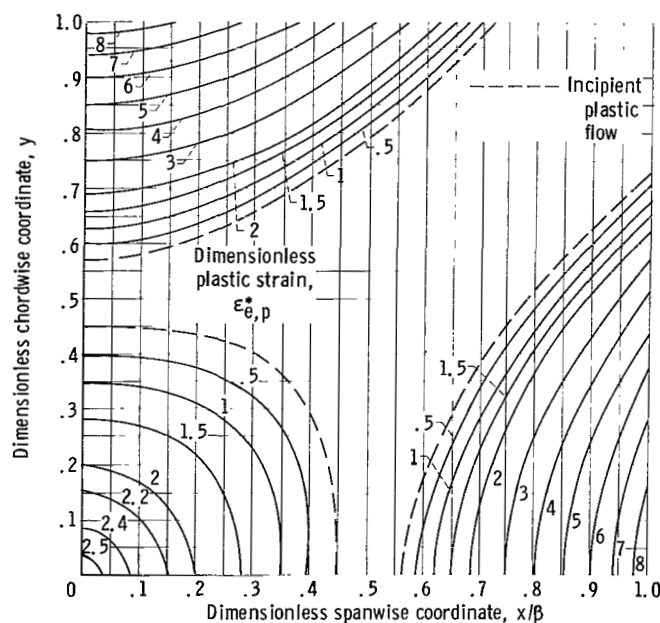


Figure 7. - Equivalent plastic strain trajectories in square plate subjected to parabolic chordwise temperature distribution.

Figure 6 compares the elastic solution throughout a square plate, as given in reference 8, with the solution of this report. There is no discernable difference.

The remainder of this section is devoted to the plastic solution for the square plate. Figure 7 shows plastic-strain trajectories for the maximum temperature distribution. The distribution is also parabolic, having the form $T^* = k_1 y^2$, with $k_1 = 20$ for this figure. It is assumed that k_1 started at some small value producing no stresses exceeding the yield point and was gradually increased to the value of 20 with no intermediate unloading. It was further assumed that there was no change in material properties with increasing temperature. The quan-

tity plotted is the summation of the increments of dimensionless equivalent plastic strain, as defined by equation (5). The curves are the loci of all points of constant equivalent plastic strain. Because of symmetry, only the first quadrant of the plate is shown. The figure discloses that for the entire plate (as opposed to the one quadrant shown in the figure) there are five regions of plastic flow. There is a region about the center almost circular in shape, being flattened at the diameters coincident with the axes of the plate;

there are four other regions, identical in shape, along the four sides of the plate. There is no plastic flow at the corners of the plate. Maximum plastic flow occurs at the centers of the four sides, where the plastic strain is roughly three times as great as at the center of the plate. Furthermore, the strain gradient is considerably steeper than that near the center.

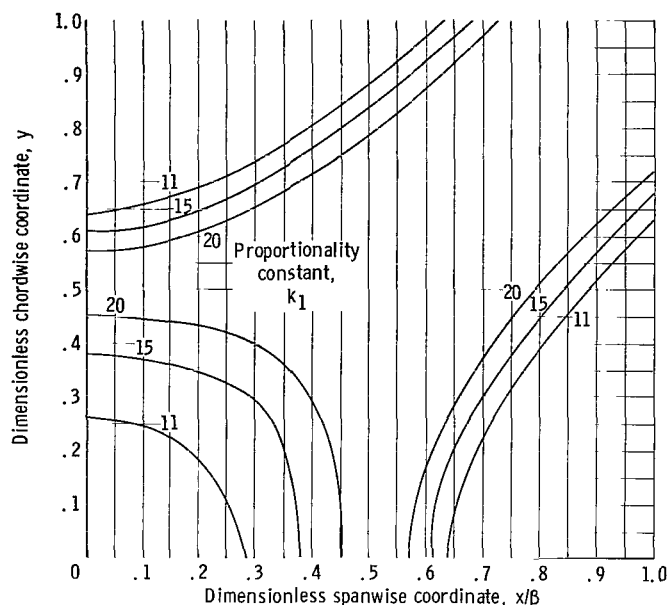


Figure 8. - Curves of incipient plastic flow at various thermal loads in square plate subjected to parabolic chordwise temperature distribution.

Figure 8 indicates the rate of growth of the regions of plastic flow. The curves are the loci of all points of incipient plastic flow for a given value of dimensionless temperature gradient. The curves, for $k_1 = 20$ are the same curves as the curves of incipient plastic flow in figure 7. Plastic flow starts first at the centers of the four sides of the plates and moves rapidly inward. Plastic flow does not start at the center of the plate until it is well developed at the sides. Once plastic flow has started at the center, however, the rate of

growth of this zone is greater than at the sides.

Ten increments of load were used to solve this problem. The increments varied between $\Delta k_1 = 1.5$ and $\Delta k_1 = 2.5$ and between $k_1 = 1.5$ (the largest value of k_1 that produces no plastic flow for a parabolic thermal gradient) and $k_1 = 20$. An experiment was run in which the increment size was gradually increased. It was found that $\Delta k_1 = 2.5$ was the largest increment that produced no significant change in the final answer. For very large increment sizes, the iterative process would not converge. It is difficult to determine, however, which is the optimum increment size for any given problem. It is also difficult to determine the optimum mesh size. Good elastic solutions were obtained with a mesh size twice as great as the 0.05 by 0.05 used for this discussion. The larger mesh, however, was too coarse for the plastic solution. Even the smaller mesh size made accurate plotting of the strain trajectories difficult. It is not known if a smaller mesh size would produce a more accurate solution, but in view of the checks discussed in the first part of this section, it is felt that this mesh size is adequate.

Murphy, in reference 9, was able to use a coarser grid. He solved a problem, however, involving proportional loading; that is, the ratios of principle stresses remained constant throughout the loading history. This permitted him to use deformation theory and presented no problem with the choice of loading increment. The choices of loading increment and grid size are interrelated. If a small loading increment is chosen, the rate of growth of the

zone of plastic flow is small, and a fine grid is necessary to detect changes in the values of plastic strain. This can be illustrated by the following example. Plastic flow first starts at the outer boundaries of the plate. As the load is gradually increased beyond the point at which localized yielding occurs, the zone of plastic flow is very small. If the grid is so coarse that the points immediately inside the plate boundary experience no plastic strain, the solution does not change in two successive iterations, and it must be concluded that convergence has occurred. In order to avoid this situation, the grid must be fine enough so that, with each increase in load, the strain at another set of points changes. Murphy did not encounter this problem because his loading increment was the final load, and many points throughout the region experienced a plastic strain.

The last matter to be discussed is an approximate method that is sometimes used in plastic flow analysis (ref. 4). This is the so-called strain invariance principle. Using this principle, an elastic analysis is made, even though it is known that plastic flow will occur. The stresses calculated will be too high at those points where yielding has occurred, but it is assumed that the calculated total strains are correct. Therefore, an approximation to the correct stresses and plastic strains may be determined by using the stress-strain curve for the material. In a multiaxial case, the equivalent strains and stresses must be used in referring to the stress-strain curve. A variation of the strain invariance assumption uses a different stress-strain curve for determining the plastic strains. It uses an ideally plastic stress-strain curve; that is, the stress-strain curve is a straight line of zero slope in the plastic region; there is no strain-hardening. The validity of these assumptions can now be investigated for the two problems under consideration.

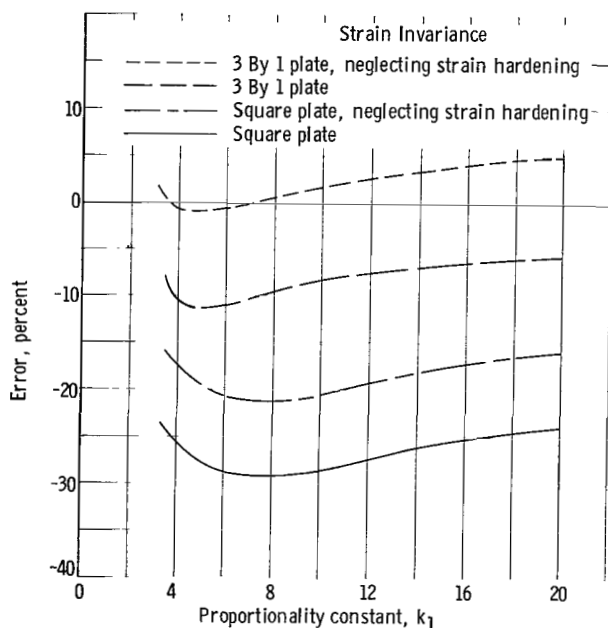


Figure 9. - Percent error in equivalent plastic strain at point of maximum strain for two approximations in long plate and short plate subjected to parabolic chordwise temperature distribution.

Shown in figure 9 is the error in the two different approximations at various loads if the finite difference solution is assumed correct. The figure is for the point of maximum plastic strain in the two plates, the mid-point of the long side. It is apparent that for both plates there is less error in the computed plastic strain when strain hardening is neglected. In the case of the long plate, where a uniaxial state of stress exists, the strain invariance approximation is quite good. In the square plate, where a biaxial stress state exists, the error is larger and nonconservative. The error, however, may be acceptable by engineering standards.

CONCLUSIONS

It has been shown that two-dimensional problems involving plastic

flow can be solved by an extension of the method of successive approximations presented in reference 4. Furthermore, comparison between available solutions indicates a high order of accuracy. It must be emphasized that the procedure utilizes basic equations of great generality. Loading history, material properties, exterior boundaries, and the stress-strain curve are all quite arbitrary.

Finally, it has been shown that the strain invariance approximation, neglecting strain-hardening, produces solutions of reasonable accuracy for two-dimensional problems. It must be noted that there is a greater error produced by that assumption in two-dimensional cases than in one-dimensional cases, and although the error is nonconservative, it may be acceptable by engineering standards.

Lewis Research Center

National Aeronautics and Space Administration
Cleveland, Ohio, August 18, 1964

APPENDIX A

MATRIX INVERSION

The solution to equation (12) is approximated by replacing the partial differential equation by a corresponding difference equation and by solving the resultant algebraic system iteratively. The equation is rewritten in the following form by first normalizing it by dividing the x-coordinate by the span-to-chord ratio β and then dividing all terms by the elastic limit σ_0 .

$$\left(\frac{1}{\beta^4} \frac{\partial^4}{\partial x^4} + \frac{2}{\beta^2} \frac{\partial^4}{\partial x^2 \partial y^2} + \frac{\partial^4}{\partial y^4} \right) \varphi^* = - \left(\frac{1}{\beta^2} \frac{\partial^2}{\partial x^2} + \frac{\partial^2}{\partial y^2} \right) T^* - g^* \quad (A1a)$$

where

$$g^* = \frac{1}{\beta^2} \frac{\partial^2}{\partial x^2} \left(\sum \Delta \epsilon_{y,p}^* + \Delta \epsilon_{y,p}^* \right) + \frac{\partial^2}{\partial y^2} \left(\sum \Delta \epsilon_{x,p}^* + \Delta \epsilon_{x,p}^* \right) - \frac{2}{\beta} \frac{\partial^2}{\partial x \partial y} \left(\sum \Delta \gamma_p^* + \Delta \gamma_p^* \right) \quad (A1b)$$

The high order difference operators are derived from the commonly used three-point first-order difference operators. For example, if $f = f(x)$ is a function of a single real variable x , then f' is its first derivative, and f'' its second derivative. By central differences,

$$f' \cong \frac{1}{2 \Delta x} (f_{k+1} - f_{k-1}) \quad (A2a)$$

$$f'' \cong \frac{1}{(\Delta x)^2} (f_{k+1} - 2f_k + f_{k-1}) \quad (A2b)$$

where k is a dummy subscript indicating the k^{th} value of f . When relations (A2) are used, the left side of equation (A1a) becomes

$$\begin{aligned} \left(\frac{1}{\beta^4} \frac{\partial^4}{\partial x^4} + \frac{2}{\beta^2} \frac{\partial^4}{\partial x^2 \partial y^2} + \frac{\partial^4}{\partial y^4} \right) \varphi^* \cong \frac{1}{\Delta^4} \left[\varphi_{i-2,j}^* + \frac{2}{\beta^2} \varphi_{i-1,j-1}^* - 4 \left(\frac{1}{\beta^2} + 1 \right) \varphi_{i-1,j}^* \right. \\ + \frac{2}{\beta^2} \varphi_{i-1,j+1}^* + \frac{1}{\beta^4} \varphi_{i,j-2}^* - 4 \left(\frac{1}{\beta^4} + \frac{1}{\beta^2} \right) \varphi_{i,j-1}^* \\ + \left(\frac{6}{\beta^4} + \frac{8}{\beta^2} + 6 \right) \varphi_{i,j}^* - 4 \left(\frac{1}{\beta^4} + \frac{1}{\beta^2} \right) \varphi_{i,j+1}^* + \frac{1}{\beta^4} \varphi_{i,j+2}^* \\ \left. + \frac{2}{\beta^2} \varphi_{i+1,j-1}^* - 4 \left(\frac{1}{\beta^2} + 1 \right) \varphi_{i+1,j}^* + \frac{2}{\beta^2} \varphi_{i+1,j+1}^* + \varphi_{i+2,j}^* \right] \quad (A3) \end{aligned}$$

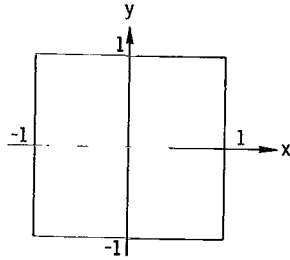


Figure 10. - Normalized coordinate system used to determine state of stress in thermally loaded thin flat plate.

where Δ is the increment of both x and y , i is the row index, and j is the column index.

The equations are written in the first quadrant of the coordinate system of figure 10. The function is defined at each intersection of a 21 by 21 point grid, as shown in figure 11. From the boundary conditions, equations (14), the value of ϕ^* is known on the boundaries (row 0 and column 21), so the equations need be written only at the intersections of the 20 by 20 point grid defined by rows 1 to 20 and columns 1 to 20. Central difference equations are used throughout by using the artifice of placing rows and columns outside the boundaries of the plate, as shown in figure 11. The boundary conditions are satisfied on the upper boundary by requiring ϕ^* to vanish on row 0, and the vanishing of the first derivative is satisfied by requiring ϕ^* on row -1 to equal ϕ^* on row 1. On the right boundary, ϕ^* on column 21 must vanish and ϕ^* on column 22 must equal ϕ^* on column 20. That is,

$$\phi_{0,j}^* = 0 \quad j = 1, \dots, 21 \quad (\text{A4a})$$

$$\phi_{i,21}^* = 0 \quad i = 0, \dots, 20 \quad (\text{A4b})$$

$$\phi_{1,j}^* = \phi_{-1,j}^* \quad j = 1, \dots, 21 \quad (\text{A4c})$$

$$\phi_{i,22}^* = \phi_{i,20}^* \quad i = 0, \dots, 20 \quad (\text{A4d})$$

Equations (A4) are equivalent to equations (13).

Similar conditions apply at the lower and left boundaries by symmetry; namely,

$$\phi_{21,j}^* = \phi_{19,j}^* \quad j = 1, \dots, 21 \quad (\text{A5a})$$

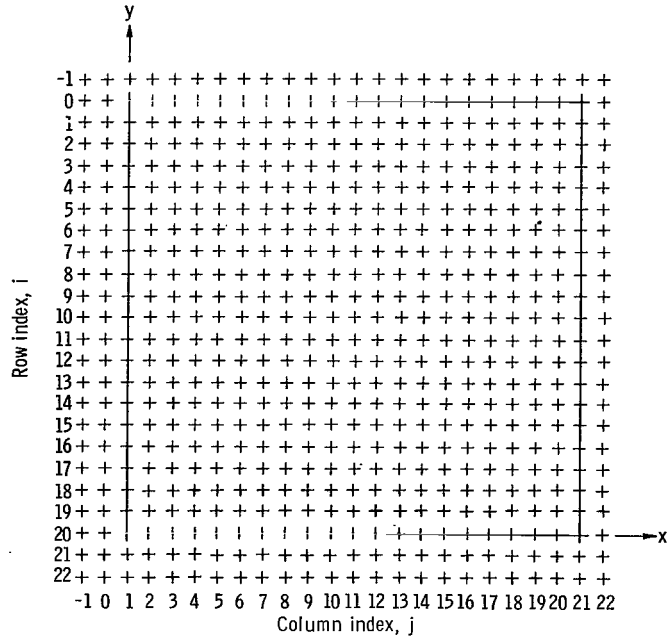


Figure 11. - Grid for difference equations.

$$\varphi_{22,j}^* = \varphi_{18,j}^* \quad j = 1, \dots, 21 \quad (\text{A5b})$$

$$\varphi_{i,0}^* = \varphi_{i,2}^* \quad i = 0, \dots, 20 \quad (\text{A5c})$$

$$\varphi_{i,-1}^* = \varphi_{i,3}^* \quad i = 0, \dots, 20 \quad (\text{A5d})$$

Note that, in the case of equations (A5), it is necessary to use two fictitious rows and columns, because the difference equations are written at points on the boundaries; whereas, in the case of equations (A4) the function φ^* is known on the boundary so that it is unnecessary to write difference equations there.

For the problem under consideration in the text, the temperature distribution is chosen so that its second derivative is a constant. The expression for g^* is written in the same way as the expression for φ^* , except that the plastic strains and their derivatives are not fully defined by the boundary conditions. Therefore, forward and backward differences are used near the boundaries instead of introducing artificial rows and columns outside the boundaries. It should be noted that this must be done for the function g^* because nothing can be said about artificial strains lying outside the boundaries.

The partial differential equation (A1) is now represented by 400 simultaneous algebraic equations. The equation is solved iteratively by guessing the values of the plastic strain increments on the right side and by solving for the values of φ^* on the left side, as discussed in the text. The coefficients of the left side do not change from iteration to iteration, so the most direct method of solving the system is to invert the coefficient matrix and multiply the inverse by the right-side column vector. The process of inversion is quite lengthy. The obvious implication is that, if many iterations are necessary, this method requires the least amount of computing time, but if few iterations are necessary, some other method is more efficient. For the problem under consideration, the former is the case.

In the process of solving the problem, 150 iterations were used for each increment of load to produce a sufficiently accurate solution; 10 loading increments were used. Had smaller loading increments been chosen, fewer iterations per increment would have been necessary, but no definite statement can be made about the total number of iterations. In fact, there is no rational procedure for determining a priori the proper increment size that will minimize the total number of iterations. Hence, it appears that the direct method of solving the system, which makes use of the inverse, is faster overall than the indirect methods discussed in reference 10. Certainly, once the inverse has been obtained, the time required for obtaining a solution for one right-side column vector is less than for any other method.

Obtaining the inverse of such a large matrix presents two major problems. The first is that of minimizing round-off errors, which can result in the loss of many significant digits due to the thousands of arithmetical operations necessary to perform the inversion. The second is the detection and correction of random errors caused by the generation of spurious bits by the calculating

machine over the long period of operating time necessary to finish the problem. These two considerations suggest the method to be used for performing the inversion.

The matrices generated by difference equations are quite sparse; that is, they contain very few nonzero elements, and these are clustered about the diagonal. This is suggested by the following illustration, which shows the 250th to the 254th rows of the matrix (the a's merely indicating nonzero elements):

209	0's,	1 a,	18 0's,	3 a's,	16 0's,	5 a's,	16 0's,	3 a's,	18 0's,	1 a,	110 0's
210	0's,	1 a,	18 0's,	3 a's,	16 0's,	5 a's,	16 0's,	3 a's,	18 0's,	1 a,	109 0's
211	0's,	1 a,	18 0's,	3 a's,	16 0's,	5 a's,	16 0's,	3 a's,	18 0's,	1 a,	108 0's
212	0's,	1 a,	18 0's,	3 a's,	16 0's,	5 a's,	16 0's,	3 a's,	18 0's,	1 a,	107 0's

It is seen that there are at most 13 nonzero elements in a row within a range of no more than 40 columns on either side of the diagonal; this suggests that the matrix be partitioned into 40 by 40 submatrices. The result is shown in figure 12. Each square represents one of the 40 by 40 submatrices. The cross-

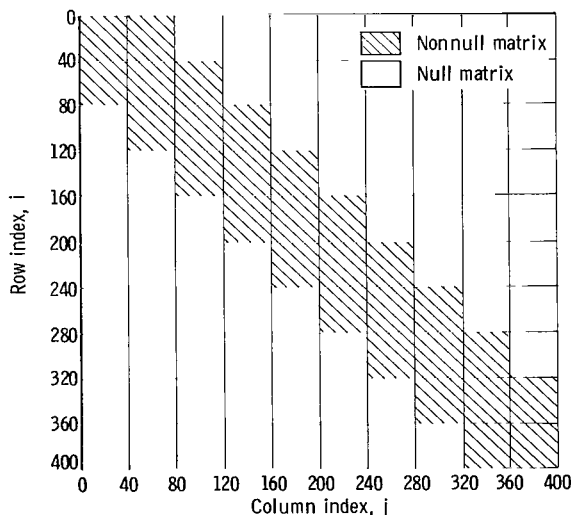


Figure 12. - Partitioned coefficient matrix.

hatched squares are the only ones containing nonzero elements; the rest are null matrices. The resulting matrix is tridiagonal and is quite simple to invert by a straightforward Gauss-Jordan elimination procedure. Furthermore, only the 28 nonnull matrices need be stored in the computer.

Several operations must be performed on the submatrices, namely, addition, multiplication, and inversion. The Crout method suggests itself immediately for inversion because it uses a check column, which permits rapid checking of the arithmetic operations at several stages of the process. This check column can also be used in the processes of matrix multiplication and addition, eliminating the problem of

spurious bit generation by the computing machine. After each matrix operation, the extra column is checked. If the check fails, the operation is repeated.

The only place where any significant round off occurs is in the process of inverting the submatrices. Reference 10 gives the following method of improving the accuracy of the elements of an inverse. Assume D_0 is an approximation to the inverse A^{-1} of a square matrix A . Then a more accurate approximation D_1 is given by

$$D_1 = D_0(2I - AD_0) \quad (A6)$$

where I is the unit matrix.

Assuming that D_0 is accurate enough to provide a good starting value, relation (A6) leads to an iterative process that will produce an inverse to any desired degree of accuracy. Experiments conducted on 40 by 40 matrices of various types showed that D_1 was accurate to at least eight significant digits when D_0 was produced by the Crout method. This permits the inversion of the 400 by 400 matrix to be performed in single precision arithmetic. After the entire inverse of the 400 by 400 matrix was obtained, a single iteration using equation (A6) was performed to improve the accuracy of its elements. The accuracy of the overall process was checked by both premultiplying and post-multiplying the 400 by 400 inverse by the original coefficient matrix and by investigating the residuals. The operation was performed in double-precision arithmetic, although it is doubtful that such care was needed for matrix multiplication. The residuals were gratifyingly small, of the order of one in the fourth place or less.

APPENDIX B

CONVERGENCE

The problem of the convergence of an iterative process is a nebulous one. It depends on the stability of the calculation procedure, the starting values chosen, the number of stations at which convergence is demanded, and the degree of accuracy desired, to mention a few of the more obvious factors. For this problem, convergence is required at six stations on the boundaries and in the interior; all were chosen because of foreknowledge of high plastic strains at these points. The degree of accuracy required is high for engineering purposes. In general, solutions accurate to better than one in the third significant digit are obtained.

Any iterative procedure is sensitive to starting values. Even in the most stable of procedures a good starting value can reduce the number of iterations required to converge to the desired degree of accuracy. In an unstable procedure, the choice of a starting value can mean the difference between converging and not converging. In a problem as lengthy as that considered in this report, any device that reduces the total computing time is worth investigating regardless of the complexity of programming. For this problem, the best guess available is that produced by the so-called strain invariance principle, as discussed in the text. Furthermore, this solution was desired, in any event, for purposes of comparison. Therefore, it was decided that these would be the starting values used.

An investigation was conducted, however, to determine precisely to what extent convergence is hastened by this procedure. The result is disappointing. Compared to starting with an initial guess of zero for all plastic-strain increments, only about 10 iterations are saved out of a total of approximately 150. The plastic-strain increments approach the converged values very rapidly in the first few iterations, and then the process slows down enormously. It is possible that, if solutions of extremely high accuracy are desired, to one unit in the fifth or sixth significant digit, for example, the process would be prohibitively long. For a problem of this type, however, it was decided that convergence to one unit in the third decimal place is more than adequate. The larger strain increments are of the order of unity, so this criterion results in better than third place accuracy in the regions of greatest strain. For normal engineering accuracy, fewer iterations would be necessary. At those stations where plastic flow is just beginning to occur, and the increment of plastic strain is quite small, the value oscillates by more than one in the third decimal place long after the larger increments have converged. Inasmuch as any error in these small increments is masked in the very next increment of loading because the next increment of plastic strain is generally at least two orders of magnitude greater, it was arbitrarily decided to stop the process after 150 iterations. Experiments were run to determine if the answers changed significantly for greater numbers of iterations, and in all cases intermediate output was investigated to ensure that the large strain increments had indeed converged and that the small ones were close to convergence. In many cases, at low loads where plastic flow is occurring at only a few points, for example,

every point converges in less than the 150 iteration limit.

The calculation procedure for determining plastic strains for a given loading increment, when stress-strain equations are used, presents certain difficulties. If plastic strains are determined from the stresses, the method is relatively unstable because the stress-strain curve is very flat in the plastic region. A small change in stress produces a large change in strain, and the procedure is quite sensitive to the size of the loading increment and to the starting values. The method of this report produces a considerable improvement in stability by calculating the increment of equivalent plastic strain from the assumed plastic-strain components and by determining equivalent stress from the stress-strain curve.

Until convergence occurs, the value of equivalent stress from the stress-strain curve does not agree with the value of equivalent stress calculated from equation (6). Thus, convergence is slowed, and again, if the loading increment is too large, the problem may diverge. In this appendix another method is presented that, in other problems of the same type as the one being discussed, has proved to be considerably more stable (converges more rapidly) and that permits the use of larger loading increments. Experiments have been conducted in which both methods were used to solve the same problem, and they converged to identical answers. This method rederives the Prandtl-Reuss equations in a form that does not contain the stresses at all, and hence does not suffer the aforementioned disadvantages. Writing the stress-strain relations for generalized plane stress in conventional x, y, z -coordinates gives

$$\epsilon_x = \frac{1}{E} (\sigma_x - \nu \sigma_y) + \alpha T + \sum_{i=1}^{n-1} \Delta \epsilon_{x,p,i} + \Delta \epsilon_{x,p,n} \quad (B1a)$$

$$\epsilon_y = \frac{1}{E} (\sigma_y - \nu \sigma_x) + \alpha T + \sum_{i=1}^{n-1} \Delta \epsilon_{y,p,i} + \Delta \epsilon_{y,p,n} \quad (B1b)$$

$$\epsilon_z = -\frac{\nu}{E} (\sigma_x + \sigma_y) + \alpha T + \sum_{i=1}^{n-1} \Delta \epsilon_{z,p,i} + \Delta \epsilon_{z,p,n} \quad (B1c)$$

$$\gamma = \frac{1 + \nu}{E} \tau + \sum_{i=1}^{n-1} \Delta \gamma_{p,i} + \Delta \gamma_{p,n} \quad (B1d)$$

When the elastic parts of the strains are designated by a superscript e , the equations can be rewritten as

$$\epsilon_x^e - \epsilon_y^e = \frac{1 + \nu}{E} (\sigma_x - \sigma_y) \quad (B2a)$$

$$\epsilon_x^e - \epsilon_z^e = \frac{1 + \nu}{E} \sigma_x \quad (\text{B2b})$$

$$\epsilon_y^e - \epsilon_z^e = \frac{1 + \nu}{E} \sigma_y \quad (\text{B2c})$$

$$\gamma^e = \frac{1 + \nu}{E} \tau \quad (\text{B2d})$$

or

$$\frac{\epsilon_x^e - \epsilon_y^e}{\sigma_x - \sigma_y} = \frac{\epsilon_x^e - \epsilon_z^e}{\sigma_x} = \frac{\epsilon_y^e - \epsilon_z^e}{\sigma_y} = \frac{\gamma^e}{\tau} = \frac{1 + \nu}{E} \quad (\text{B3})$$

A modified total strain is now defined as follows:

$$\epsilon_x' \equiv \epsilon_x - \sum_{i=1}^{n-1} \Delta\epsilon_{x,p,i} = \epsilon_x^e + \alpha T + \Delta\epsilon_{x,p,n} \quad (\text{B4a})$$

$$\epsilon_y' \equiv \epsilon_y - \sum_{i=1}^{n-1} \Delta\epsilon_{y,p,i} = \epsilon_y^e + \alpha T + \Delta\epsilon_{y,p,n} \quad (\text{B4b})$$

$$\epsilon_z' \equiv \epsilon_z - \sum_{i=1}^{n-1} \Delta\epsilon_{z,p,i} = \epsilon_z^e + \alpha T + \Delta\epsilon_{z,p,n} \quad (\text{B4c})$$

$$\gamma' \equiv \gamma - \sum_{i=1}^{n-1} \Delta\gamma_{p,i} = \gamma^e + \Delta\gamma_{p,n} \quad (\text{B4d})$$

The basic assumption of Prandtl is that, at any instant of loading in the plastic range, the plastic-strain increments are proportional to the respective instantaneous stress deviations, which in the notation of this paper is equivalent to

$$\frac{\Delta\epsilon_{x,p} - \Delta\epsilon_{y,p}}{\sigma_x - \sigma_y} = \frac{\Delta\epsilon_{x,p} - \Delta\epsilon_{z,p}}{\sigma_x} = \frac{\Delta\epsilon_{y,p} - \Delta\epsilon_{z,p}}{\sigma_y} = \frac{\Delta\gamma_p}{\tau} = \Delta\lambda \quad (\text{B5})$$

where $\Delta\lambda$ is an instantaneous nonnegative constant of proportionality, which may vary throughout the loading program. Combining equations (B3) to (B5) yields

$$\frac{\Delta\epsilon_{x,p} - \Delta\epsilon_{y,p}}{\epsilon_x' - \epsilon_y'} = \frac{\Delta\epsilon_{x,p} - \Delta\epsilon_{z,p}}{\epsilon_x' - \epsilon_z'} = \frac{\Delta\epsilon_{y,p} - \Delta\epsilon_{z,p}}{\epsilon_y' - \epsilon_z'} = \frac{\Delta\gamma_p}{\gamma'} = \frac{\Delta\lambda}{\Delta\lambda + \frac{1 + \nu}{E}} \equiv K \quad (\text{B6})$$

where K is a constant. From this it follows that

$$\begin{aligned} & (\Delta\epsilon_{x,p} - \Delta\epsilon_{y,p})^2 + (\Delta\epsilon_{x,p} - \Delta\epsilon_{z,p})^2 + (\Delta\epsilon_{y,p} - \Delta\epsilon_{z,p})^2 + 6\Delta\gamma_p^2 \\ & = K^2 \left[(\epsilon'_x - \epsilon'_y)^2 + (\epsilon'_x - \epsilon'_z)^2 + (\epsilon'_y - \epsilon'_z)^2 + 6(\gamma')^2 \right] \end{aligned} \quad (B7)$$

Defining

$$\Delta\epsilon_{e,p} \equiv \frac{\sqrt{2}}{3} \sqrt{(\Delta\epsilon_{x,p} - \Delta\epsilon_{y,p})^2 + (\Delta\epsilon_{x,p} - \Delta\epsilon_{z,p})^2 + (\Delta\epsilon_{y,p} - \Delta\epsilon_{z,p})^2 + 6\Delta\gamma_p^2} \quad (B8)$$

and

$$\epsilon_{e,t} \equiv \frac{\sqrt{2}}{3} \sqrt{(\epsilon'_x - \epsilon'_y)^2 + (\epsilon'_x - \epsilon'_z)^2 + (\epsilon'_y - \epsilon'_z)^2 + 6(\gamma')^2} \quad (B9)$$

yields

$$K = \frac{\Delta\lambda}{\Delta\lambda + \frac{1+\nu}{E}} = \frac{\Delta\epsilon_{e,p}}{\epsilon_{e,t}} \quad (B10)$$

Making use of the incompressibility assumption

$$\epsilon_{x,p} + \epsilon_{y,p} + \epsilon_{z,p} = 0 \quad (B11)$$

and solving equation (B6) for the individual strain increments yield

$$\Delta\epsilon_{x,p} = \frac{\Delta\epsilon_{e,p}}{3\epsilon_{e,t}} (2\epsilon'_x - \epsilon'_y - \epsilon'_z) \quad (B12a)$$

$$\Delta\epsilon_{y,p} = \frac{\Delta\epsilon_{e,p}}{3\epsilon_{e,t}} (2\epsilon'_y - \epsilon'_x - \epsilon'_z) \quad (B12b)$$

$$\Delta\epsilon_{z,p} = -\Delta\epsilon_{x,p} - \Delta\epsilon_{y,p} \quad (B12c)$$

$$\Delta\gamma_p = \frac{\Delta\epsilon_{e,p}}{\epsilon_{e,t}} \gamma' \quad (B12d)$$

Now all that remains is to relate the values of $\Delta\epsilon_{e,p}$ and $\epsilon_{e,t}$ to the stress-strain curve. Combining the relations for $\Delta\lambda$ (eq. (B5)), equivalent plastic-strain increment (eq. (B8)), and equivalent stress (eq. (6)) yields

$$\Delta\lambda = \frac{3}{2} \frac{\Delta\epsilon_{e,p}}{\sigma_e} \quad (B13)$$

Combining equations (B10) and (B13) produces

$$\epsilon_{e,t} = \Delta\epsilon_{e,p} + \frac{2}{3} \frac{1+\nu}{E} \sigma_e \quad (\text{B14})$$

Let the value of σ_e at the end of any given loading increment be designated by $\sigma_{e,i}$ and the value at the end of the preceding increment be designated by $\sigma_{e,i-1}$. An expression for σ_e can then be written in a Taylor series and approximated as follows if terms of high order are neglected and differential operators are replaced with difference operators:

$$\sigma_{e,i} \cong \sigma_{e,i-1} + \left(\frac{\Delta\sigma_e}{\Delta\epsilon_{e,p}} \right)_{i-1} \Delta\epsilon_{e,p} \quad (\text{B15})$$

Combining equations (B14) and (B15) yields

$$\Delta\epsilon_{e,p} = \frac{\epsilon_{e,t} - \frac{2}{3} \frac{1+\nu}{E} \sigma_{e,i-1}}{1 + \frac{2}{3} \frac{1+\nu}{E} \left(\frac{\Delta\sigma_e}{\Delta\epsilon_{e,p}} \right)_{i-1}} \quad (\text{B16})$$

Thus, a strain-strain relation can be derived from a stress-strain curve by using equation (B16). It is to be noted that, for linear strain-hardening, equation (B16) is exact. Inasmuch as most stress-strain curves are nearly flat, equation (B16) is very nearly exact; and the strain-strain curve is very nearly a straight line having a slope of unity. Therefore, an iterative process utilizing the strain-strain curve is more rapidly convergent than one utilizing the stress-strain curve. The iterative procedure for determining the plastic-strain increments is as follows:

- (1) Obtain elastic solution.
- (2) Guess plastic-strain increments.
- (3) Calculate the corresponding "modified" total strains from equations (B4) and evaluate $\epsilon_{e,t}$ from (B9).
- (4) Find $\Delta\epsilon_{e,p}$ from equation (B16).
- (5) Calculate a new set of plastic-strain increments from equations (B12).
- (6) Repeat steps 3 to 5 until succeeding values of plastic-strain increments are sufficiently close to each other. It is to be noted that, as convergence is approached, the value of $\Delta\epsilon_{e,p}$ produced from equation (B16) approaches the value calculated from equation (B8).

REFERENCES

1. Manson, S. S.: Behavior of Materials Under Conditions of Thermal Stress. NACA TN 2933, 1953.
2. Hill, R.: The Mathematical Theory of Plasticity. Clarendon Press (Oxford), 1950.
3. Mendelson, A., and Spero, S. W.: A General Solution for the Elastoplastic Thermal Stresses in a Strain-Hardening Plate with Arbitrary Material Properties. Jour. Appl. Mech., vol. 29, no. 1, Mar. 1962, pp. 151-158.
4. Mendelson, A., and Manson, S. S.: Practical Solution of Plastic Deformation Problems in Elastic-Plastic Range. NASA TR R-28, 1959.
5. de G. Allen, D. N., and Southwell, R.: Relaxation Methods Applied to Engineering Problems. XIV. Plastic Straining in Two-Dimensional Stress-Systems. Phil. Trans. Roy. Soc. (London), sec. A, vol. 242, no. 850, June 7, 1950, pp. 379-414.
6. Sokolnikoff, I. S.: Mathematical Theory of Elasticity. McGraw-Hill Book Co., Inc., 1956.
7. Mendelson, Alexander, and Hirschberg, Marvin: Analysis of Elastic Thermal Stresses in Thin Plate with Spanwise and Chordwise Variations of Temperature and Thickness. NACA TN, 3778, 1956.
8. Roberts, Ernest, Jr., and Mendelson, Alexander: A Simplified Method of Determining the Elastic State of Thermal Stress in a Thin, Flat Plate of Finite Dimensions. NASA TN, D-1740, 1963.
9. Murphy, J. H.: Thermal Stresses In a Rectangular Plate. Ph.D. Thesis, Georgia Inst. Tech., 1962.
10. Faddeeva, V. N.: Computational Methods of Linear Algebra. Dover Pub., Inc., 1959.

2/1/85
08

"The aeronautical and space activities of the United States shall be conducted so as to contribute . . . to the expansion of human knowledge of phenomena in the atmosphere and space. The Administration shall provide for the widest practicable and appropriate dissemination of information concerning its activities and the results thereof."

—NATIONAL AERONAUTICS AND SPACE ACT OF 1958

NASA SCIENTIFIC AND TECHNICAL PUBLICATIONS

TECHNICAL REPORTS: Scientific and technical information considered important, complete, and a lasting contribution to existing knowledge.

TECHNICAL NOTES: Information less broad in scope but nevertheless of importance as a contribution to existing knowledge.

TECHNICAL MEMORANDUMS: Information receiving limited distribution because of preliminary data, security classification, or other reasons.

CONTRACTOR REPORTS: Technical information generated in connection with a NASA contract or grant and released under NASA auspices.

TECHNICAL TRANSLATIONS: Information published in a foreign language considered to merit NASA distribution in English.

TECHNICAL REPRINTS: Information derived from NASA activities and initially published in the form of journal articles.

SPECIAL PUBLICATIONS: Information derived from or of value to NASA activities but not necessarily reporting the results of individual NASA-programmed scientific efforts. Publications include conference proceedings, monographs, data compilations, handbooks, sourcebooks, and special bibliographies.

Details on the availability of these publications may be obtained from:

SCIENTIFIC AND TECHNICAL INFORMATION DIVISION
NATIONAL AERONAUTICS AND SPACE ADMINISTRATION
Washington, D.C. 20546